AGU PUBLICATIONS

JGR

Journal of Geophysical Research: Earth Surface

INTRODUCTION TO A SPECIAL SECTION

10.1002/2015JF003518

Special Section:
Glacier Surging and Ice Streaming

Key Points:
- Changes in ice flow velocity are recorded within Institute Ice Stream (IIS) tributaries
- Holocene flow reconfiguration was facilitated by enhanced flow through two IIS tributaries
- IIS tributaries acted as a source area for former ice streaming over Bungenstock Ice Rise

Supporting Information:
- Figure S1

Correspondence to:
K. Winter,
kate.winter@northumbria.ac.uk

Citation:
Winter, K., J. Woodward, N. Ross, S. A. Dunning, R. G. Bingham, H. F. J. Corr, and M. J. Siegert (2015), Airborne radar evidence for tributary flow switching in Institute Ice Stream, West Antarctica: Implications for ice sheet configuration and dynamics, *J. Geophys. Res. Earth Surf.*, *120*, doi:10.1002/2015JF003518.

Received 28 FEB 2015
Accepted 26 JUL 2015
Accepted article online 3 AUG 2015

©2015. The Authors.
This is an open access article under the terms of the Creative Commons Attribution License, which permits use, distribution and reproduction in any medium, provided the original work is properly cited.

Airborne radar evidence for tributary flow switching in Institute Ice Stream, West Antarctica: Implications for ice sheet configuration and dynamics

Kate Winter[1], John Woodward[1], Neil Ross[2], Stuart A. Dunning[1], Robert G. Bingham[3], Hugh F. J. Corr[4], and Martin J. Siegert[5]

[1]Department of Geography, Faculty of Engineering and Environment, Northumbria University, Newcastle upon Tyne, UK, [2]School of Geography, Politics and Sociology, Newcastle University, Newcastle upon Tyne, UK, [3]School of Geosciences, University of Edinburgh, Edinburgh, UK, [4]British Antarctic Survey, Cambridge, UK, [5]Grantham Institute and Department of Earth Science and Engineering, Imperial College London, London, UK

Abstract Despite the importance of ice streaming to the evaluation of West Antarctic Ice Sheet (WAIS) stability we know little about mid- to long-term dynamic changes within the Institute Ice Stream (IIS) catchment. Here we use airborne radio echo sounding to investigate the subglacial topography, internal stratigraphy, and Holocene flow regime of the upper IIS catchment near the Ellsworth Mountains. Internal layer buckling within three discrete, topographically confined tributaries, through Ellsworth, Independence, and Horseshoe Valley Troughs, provides evidence for former enhanced ice sheet flow. We suggest that enhanced ice flow through Independence and Ellsworth Troughs, during the mid-Holocene to late Holocene, was the source of ice streaming over the region now occupied by the slow-flowing Bungenstock Ice Rise. Although buckled layers also exist within the slow-flowing ice of Horseshoe Valley Trough, a thicker sequence of surface-conformable layers in the upper ice column suggests slowdown more than ~4000 years ago, so we do not attribute enhanced flow switch-off here, to the late Holocene ice-flow reorganization. Intensely buckled englacial layers within Horseshoe Valley and Independence Troughs cannot be accounted for under present-day flow speeds. The dynamic nature of ice flow in IIS and its tributaries suggests that recent ice stream switching and mass changes in the Siple Coast and Amundsen Sea sectors are not unique to these sectors, that they may have been regular during the Holocene and may characterize the decline of the WAIS.

1. Introduction

Institute Ice Stream (IIS) (81.5°S, 75°W), a major outlet for the West Antarctic Ice Sheet (WAIS), drains into the Filchner-Ronne Ice Shelf (FRIS) in the Weddell Sea sector of West Antarctica (Figure 1). However, despite IIS being critical to our evaluation of WAIS stability and the likelihood of future sea level change from ice sheet loss [*Bentley et al.*, 2010], dynamic former changes in ice flow within the ice stream's catchment area are poorly constrained. IIS and neighboring Möller Ice Stream (MIS) currently drain a combined area of 218,000 km^2 [*Joughin and Bamber*, 2005], ~11% of the WAIS total. They discharge into the FRIS on either side of Bungenstock Ice Rise (Figure 2). Both IIS and MIS have steep reverse bed slopes and areas of low basal roughness which could make them susceptible to unstable grounding line retreat [*Ross et al.*, 2012; *Wright et al.*, 2014]. Theories of historic grounding line retreat and/or an expanding ice sheet in the Weddell Sea sector of the WAIS during the Holocene have recently been proposed by *Siegert et al.* [2013] and in part tested by *Bradley et al.* [2015]. Surface flow stripes on Bungenstock Ice Rise (Figure 2b) have led to the suggestion that an adjustment to the flow path of IIS could have occurred during a phase of ice sheet retreat or by an advance of the grounding line from an already retreated situation that existed approximately 400–4000 years ago. Modeling studies have suggested that a migration of IIS occurred during the last deglaciation [*Fogwill et al.*, 2014] and that future changes in mass balance may lead to rapid grounding line retreat [*Wright et al.*, 2014].

Similar short-term (century scale) variability in ice-flow direction and discharge have been recognized within several other Antarctic ice streams [*Anandakrishnan and Alley*, 1997; *Conway et al.*, 2002; *Siegert et al.*, 2003],

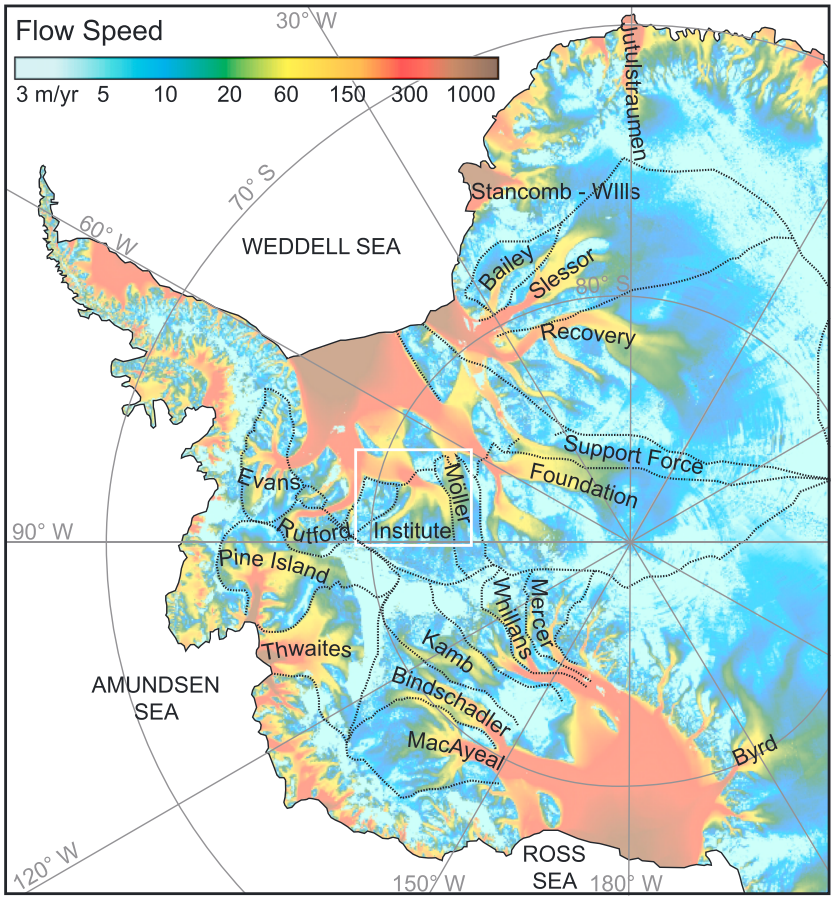

Figure 1. Satellite-derived surface ice-flow velocities of the Antarctic Ice Sheet from MEaSUREs [*Rignot et al.*, 2011a], annotated to show dominant ice streams and their catchment areas. The white box indicates the locations of Figures 2a, 2c, 2d, 9a, and 9b.

including those on the Siple Coast (Ross Sea sector) where the ice streams have a comparable basal topography to those draining into the FRIS. Since the Last Glacial Maximum (LGM), which occurred sometime between 29 and 33 ka in West Antarctica [*Clark et al.*, 2009], the Siple Coast ice streams have experienced more than 1200 km of grounding line retreat, accompanied by significant mass loss which has resulted in significant drainage-basin reconfiguration and flow switching [*Hulbe and Fahnestock*, 2007; *Conway et al.*, 2002; *Catania et al.*, 2006].

To improve the forecasting of the WAIS response to future climate forcing it is critical that historic ice sheet dynamics are understood and indeed, better represented in the next generation of ice sheet models [*Vaughan et al.*, 2013]. Detailed investigations in the Ross and Amundsen Sea sectors have greatly improved the understanding of recent dynamic ice stream switching and drawdown in the Pacific sector of the WAIS, but more work is needed on the Atlantic (i.e., Weddell Sea) sector of West Antarctica. To determine the likelihood of historic ice-flow reorganization in the upper IIS catchment and former flow conditions this study uses airborne radio echo sounding (RES) to ascertain the subglacial topography and internal layering of the ice sheet in and around the Ellsworth Subglacial Highlands.

2. Study Area

Draining 151,000 km^2, IIS catchment is one of the largest in West Antarctica (Figure 1). The catchment borders the southern lobe of the Pine Island Glacier drainage system, the southern catchment of Rutford Ice Stream, and the uppermost part of Bindschadler Ice Stream catchment. To the east it is bounded by MIS (82.5°S, 71°W), and to the west the boundary is controlled by the high bedrock topography of the Ellsworth Mountains

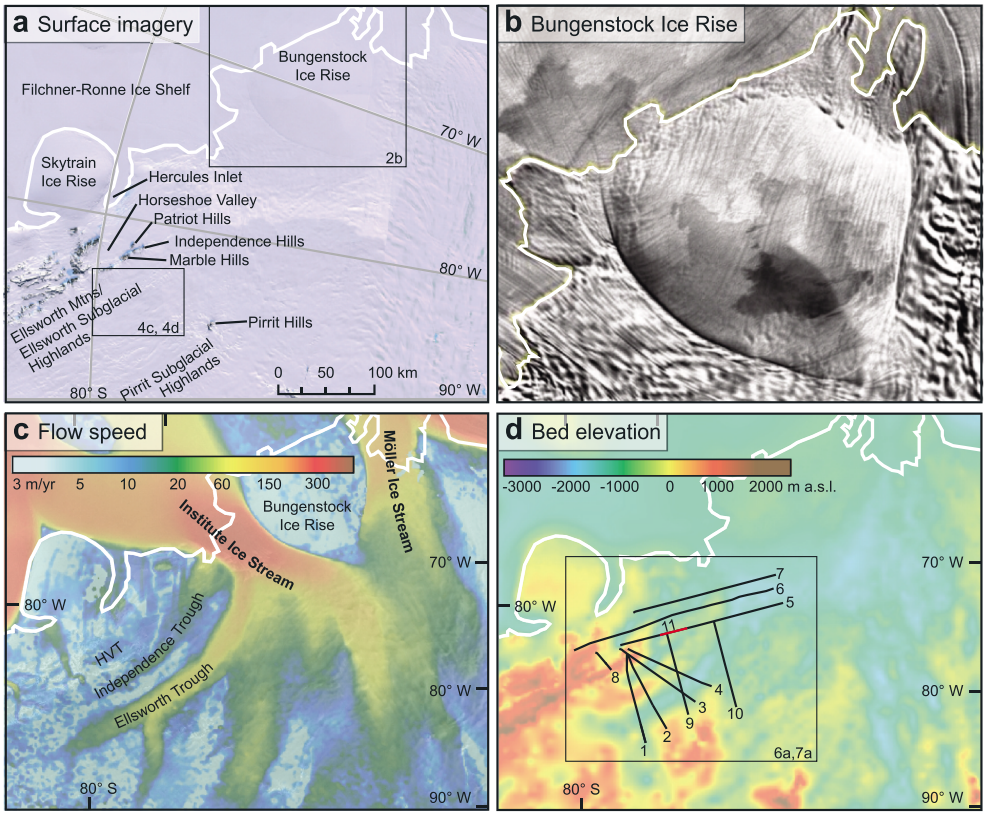

Figure 2. (a) Moderate Resolution Imaging Spectroradiometer (MODIS) and Landsat Image Mosaic of Antarctica (LIMA) mosaic with prominent geographical features labeled; the labeled boxes outline the location of Figures 2b and 4c/4d, and the white line indicates the ASAID grounding line [*Bindschadler et al.*, 2011]. (b) MODIS mosaic of surface lineations on Bungenstock Ice Rise [*Haran et al.*, 2006]; the white line indicates the ASAID grounding line [*Bindschadler et al.*, 2011]. (c) Satellite-derived surface ice-flow velocities from MEaSUREs [*Rignot et al.*, 2011a] superimposed over MODIS satellite imagery [*Haran et al.*, 2006] and annotated to show dominant ice streams, Bungenstock Ice Rise, Horseshoe Valley Trough (HVT), Independence Trough, and Ellsworth Trough; the white line indicates the ASAID grounding line [*Bindschadler et al.*, 2011]. (d) Location of RES data used in this paper. Background shows bed elevation from the same area as Figures 2a and 2c, derived from Bedmap2 [*Fretwell et al.*, 2013]; the white line indicates the ASAID grounding line [*Bindschadler et al.*, 2011].

(80°S, 81°W). Approximately 60% of the catchment lies below sea level and is characterized by a diverse subglacial topography exemplified by the deep incised valleys and subglacial ridges that lie between the Ellsworth Subglacial Highlands and the Pirrit Subglacial Highlands.

The ice that currently flows across the grounding line through IIS is sourced from two flow units. One is the ice that comes from the broad upper IIS catchment that adjoins the Siple Coast ice streams. The second, which is the focus of this paper, comprises a series of tributaries around, and west of, the Ellsworth Mountains. The mountains are characterized by a series of high-amplitude geological folds, which define tectonically controlled subbasins and the steep mountain ranges of the Patriot, Marble, and Independence Hills [*Jordan et al.*, 2013] (Figure 2a). These ranges reach elevations in the region of 1200–1600 m above sea level and approximately 150–300 m above the present ice surface. This geological template acts as a strong control on the past, present, and future configuration of ice flow in this area. In particular, we focus on the ice flowing through three distinct geological troughs in the Ellsworth Subglacial Highlands, namely, Horseshoe Valley Trough (named after "Horseshoe Valley" at its head), Independence Trough, and Ellsworth Trough (Figure 2).

3. Methods

3.1. Radar Survey and Processing

Over 4000 km of airborne RES data, collected during a survey of IIS and MIS in austral summer 2010/2011, have been analyzed. Flights were flown in a stepped pattern to optimize the acquisition of gravity data

[*Ross et al*., 2012]. The British Antarctic Survey Polarimetric-radar Airborne Science Instrument (PASIN) ice-sounding radar [*Corr et al*., 2007] operates at a frequency of 150 MHz and a bandwidth of 12 MHz, with a pulse-coded waveform acquisition rate of 312.5 Hz. Flight altitude was compensated for using radar/laser altimeter terrain-clearance measurements, with aircraft position obtained from differential global positioning systems. Internal layering cannot be resolved within the southwestern side of Horseshoe Valley Trough as aircraft took off and/or landed in front of Patriot Hills. The uppermost 200 samples of the ice column are poorly resolved in all radagrams, as a function of 2-D synthetic aperture radar (SAR) processing. All RES data were preprocessed using Doppler (SAR) processing which was 2-D focused. The initial processing was employed to migrate radar-scattering hyperbolae in the along-track direction, before the data were further processed (natural logarithm applied to enhance weaker reflections) and displayed in ReflexW [*Sandmeier Scientific Software*, 2012], version 6.1.1. Conversion of time to depth was achieved by application of a constant two-way travel time of 0.168 m ns^{-1} offset by a nominal value of 10 m to correct for the firn layer [*Ross et al*., 2012]. Based on crossover analysis of the entire survey, RMS differences of 1.44 m were found in ice surface elevation and 18.29 m in ice thickness measurements, although an RMS error of 20.58 m was obtained for the upper parts of the gridded survey area, which is in part caused by the roughness of the underlying topography [*Ross et al*., 2012]. Technical details of the PASIN system are available in *Corr et al*. [2007], and additional details on the acquisition and processing of the data are provided in *Ross et al*. [2012].

3.2. Analysis of Internal Layering

Internal layers in the ice sheet are the result of variations in the density, conductivity, or crystal fabric of the ice. Formed initially through surface accumulation and modified by subsequent burial, compaction, and ice flow, they are recorded in radargrams because they are spatially coherent boundaries in the dielectric properties of the ice and thus reflect a small fraction of the radar signal [*Drews et al*., 2013]. Previous studies by *Rippin et al*. [2003], *Siegert et al*. [2003], *Bingham et al*. [2007], and *Karlsson et al*. [2009] have used internal layering to investigate the internal structure of the ice sheet and its relationship with present or past ice-flow velocity. Following these studies the classification of internal layers has been divided into two main types: (1) continuous, well-defined layering comprises internal layers which predominantly follow the surface and/or bed topography and (2) discontinuous, buckled or disrupted layering which denotes internal-layer geometries that substantially diverge from the bed and/or surface. Continuous layering is primarily located in regions which currently experience or have experienced slow-flowing ice, defined here as ice flow <30 m a^{-1} which has undergone little motion. In contrast, disrupted layering is often coincident with areas that have previously encountered or are currently experiencing fast flow (defined here as >30 m a^{-1}) or at the boundary between areas of slow and enhanced flow [*Karlsson et al*., 2009]. For this paper, we generally specify the term "enhanced flow" as distinct from the term "fast flow" because the latter term is often equated with more extreme ice speeds in ice streams. Previous studies [e.g., *Bingham et al*., 2007] have shown that the more modest speeds attained by ice stream tributaries are all that is required to produce the disruptions to internal layering.

Interpretations of the internal stratigraphy of IIS have followed two established approaches, which work at different scales: (1) manual, qualitative interpretations have been used for detailed analysis of RES data in Figures 3–7, while (2) automated, quantitative interpretations have been used to examine the extended RES data set in Figure 8. The first approach highlights internal stratigraphy through manual digitization of radargrams, where strongly reflective horizons were marked by black solid lines, while internal features with reduced reflectivity were marked with dashed lines (as their exact form was harder to define). The purple lines were used to extrapolate internal stratigraphic features in areas where radar returns were low. The second approach uses an Internal Layering Continuity Index (ILCI), which has been employed to characterize regions of apparently continuous versus disrupted internal layering from large-scale RES data sets. The ILCI, developed by *Karlsson et al*. [2012], and recently applied to the wider catchments of IIS and MIS by *Bingham et al*. [2015], uses A-scope plots of each RES trace (each trace representing a stack of 10 consecutive raw traces to minimize noise [*Karlsson et al*., 2012]) to record peaks of high reflected relative power, bounded by values of lower reflected relative power. Using the relative changes in power (uniform in value across all study sites) the continuity of internal layers can be determined, as areas with clear internal layers return a high continuity index (0.06–0.10), while A scopes interrogated, where layering is absent, return a low continuity index (0–0.03). This leaves disrupted internal layering to return an intermediate value (0.03–0.06). These low and

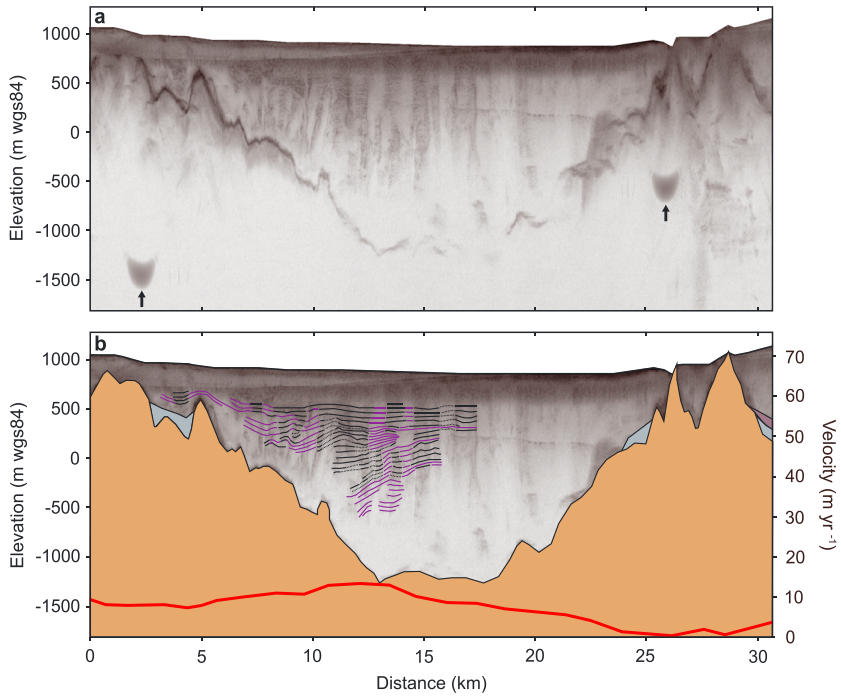

Figure 3. (a) Radio echo sounding cross section of Horseshoe Valley Trough (line 8); the arrows indicate processing artifacts. b) Digitized basal topography (brown), lower basal ice unit (blue) and upper basal ice unit (purple) as well as internal stratigraphic features (black for observed, dashed for inferred, and purple for best estimate). The secondary axis shows satellite-derived surface ice-flow velocities in red from MEaSUREs [*Rignot et al.*, 2011a].

intermediate values have been interpreted to represent present or previously enhanced flow which is characterized by disrupted layer packages interspersed with regions of little to no layering.

3.3. Surface Velocity Data

Surface velocity data were acquired from the NASA Making Earth System Data Records for Use in Research Environments (MEaSUREs) interferometric synthetic aperture radar-based Antarctica ice velocity map [*Rignot et al.*, 2011a]. The digital mosaic was created using ALOS PALSAR, RADARSAT-1, RADARSAT-2, ERS-1, ERS-2, and Envisat advanced synthetic aperture radar sensors, which each covered discrete areas of Antarctica from 1996 to 2009 [*Rignot et al.*, 2011b]. Nominal errors, associated with the precision of ice-flow mapping, exist and vary within the digital mosaic depending on data collection methods, the type of instrument used, the geographic location, the time period and repeat cycle of the instrument, as well as the amount of data stacking. Using the error map from *Rignot et al.* [2011b] we estimate the precision of ice-flow mapping in our study area to be 4.2 m a^{-1}.

4. Results

4.1. Basal Topography

Radar observations of IIS's upper catchment, in and around the Ellsworth Subglacial Highlands, reveal a complex tectonically controlled basal topography [*Jordan et al.*, 2013; *Ross et al.*, 2014] with multiple nunataks, buried mountains, highland plateaus, basins, and troughs. The 20 km wide Horseshoe Valley Trough (Figure 3) is confined, in its upper parts, by the steep mountains of the Heritage Range, as well as a subglacial ridge which is situated between the mouth of Horseshoe Valley and the present-day trunk of IIS. With a smooth bed lying 1300 m below sea level, Horseshoe Valley Trough contains an ice column in excess of 2000 m. However, the ice sheet thickness reduces significantly, to just 750 m, as the ice flows out of Horseshoe Valley where it is deflected northward over higher-elevation terrain toward the main trunk of IIS (Figure 2).

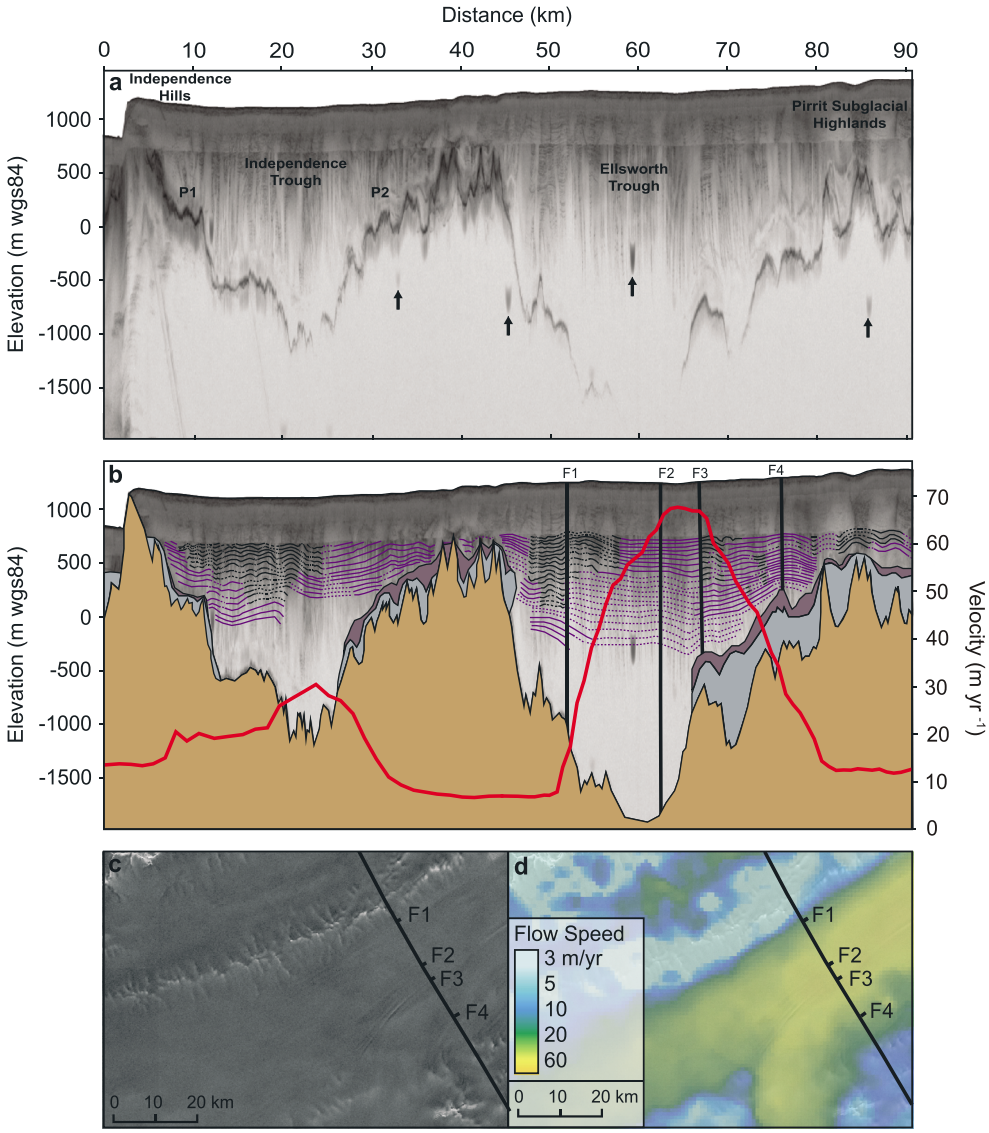

Figure 4. (a) Radio echo sounding cross section of Independence and Ellsworth Troughs (line 2); the arrows indicate processing artifacts. (b) Digitized basal topography (brown), lower basal ice unit (blue), and upper basal ice unit (purple) as well as internal stratigraphic features (black for observed, dashed for inferred, and purple for best estimate) and the location of surface flow stripes (F1–F4). The secondary axis highlights satellite-derived surface ice-flow velocities in red from MEaSUREs [*Rignot et al*., 2011a]. (c) Flow stripes (F1–F4) annotated from RADARSAT mosaic [*Haran et al*., 2006]. (d) Flow stripes identified on a satellite-derived surface ice-flow velocity map from MEaSUREs [*Rignot et al*., 2011a].

Lying subparallel to Horseshoe Valley Trough, but separated from it by the 1400 m peaks of Independence Hills (Figure 2), is Independence Trough which is delineated to the south by a 20 km wide subglacial mountain range which has a maximum elevation of 770 m above present sea level (Figure 4). The ~22 km wide trough has a distinctive morphology which is defined by the existence of two plateaus (P1 and P2 in Figure 4), each ~6 km wide and running parallel to the main axis of the trough, breaking the steep slope from the nunataks of Independence Hills to the deep valley floor which lies 1100 m below sea level (Figure 4). For 54 km, along its long axis from its head, the trough remains deep and straight until the ice begins to flow in a more northward direction, where the now 50 km wide, 2200 m thick ice flow is contained by approximately parallel high-elevation subglacial plateaus until reaching the main trunk of the IIS where the ice flow crosses the grounding line (Figure 2c).

Described in detail by *Ross et al*. [2014], Ellsworth Trough (Figure 4) is the widest and most extensive valley to be surveyed (up to a maximum of 34 km wide and 260 km in length; Figure 2c). Although steep-sided

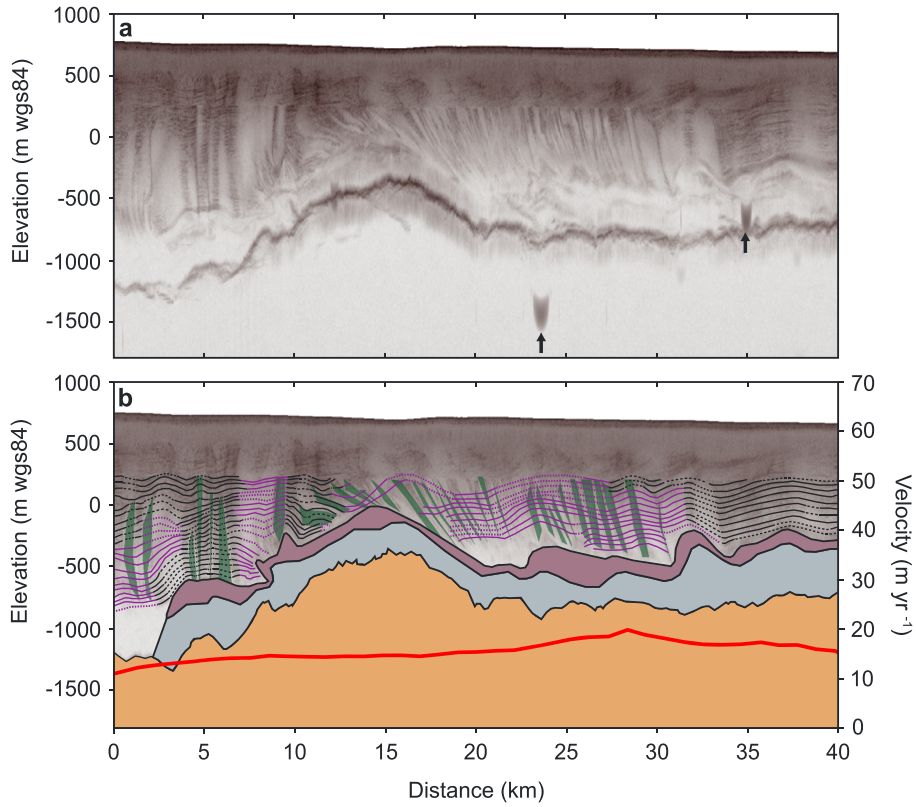

Figure 5. (a) Selected internal features in radio echo sounding flight line 11; the arrows indicate a processing artifact. (b) Digitized basal topography (brown), lower basal ice unit (blue), and upper basal ice unit (purple) as well as internal stratigraphic features (black for observed, dashed for inferred, and purple for best estimate); the green polygons show the location of internal whirlwinds. The secondary axis highlights satellite-derived surface ice-flow velocities in red from MEaSUREs [*Rignot et al.*, 2011a].

bedrock walls confine the northern flank of the trough, the southern walls feature a more gradual inclination toward a high-elevation subglacial plateau (Figure 4). Here the mountainous basal topography is intersected by a number of smaller valleys which are orientated roughly perpendicular to the main trough axis and present-day ice flow. Two major tributaries feed Ellsworth Trough at the point where the trough becomes straight and aligned with Independence Trough (Figure 2c). Here ice thicknesses of 2100 m–2620 m are recorded as the ice is funneled northward toward IIS, above bed elevations of 700 m–1500 m below sea level.

4.2. Internal Stratigraphy

The RES data reveal several englacial features qualitatively interpreted to be related to ice dynamics. These include basal units lacking evidence for clear internal ice sheet layering, continuous and discontinuous internal layers, highly disrupted internal layers, and low-reflectivity structures which resemble "whirlwinds" or "tornados" [*Karlsson et al.*, 2009]. The latter are visible in radargrams throughout the study area, in a variety of radar flight-line orientations. An example of these whirlwinds is shown in Figure 5 (although also visible in Figures 3, 4, 6, and 7, the larger scales used in these figures, which were chosen for regional analysis, are not appropriate for marking the locations of whirlwind features). In Figure 5, and indeed, within numerous other radargrams from the study, englacial layering is disrupted and occasionally obliterated by vertical to subvertical low-reflectivity zones. These features are the complex response of the radar signal to high-amplitude buckling of layers within the ice sheet (i.e., physical ice sheet features that present in the radargrams as whirlwinds [*Holschuh et al.*, 2014]). The whirlwinds can therefore be used to identify and map zones of buckled and disrupted layering.

Basal ice units are apparent above the bed in multiple radargrams (Figures 3–5). These basal units, identified across the study area, are clearly distinguishable from the bed and the upper ice column, where they can

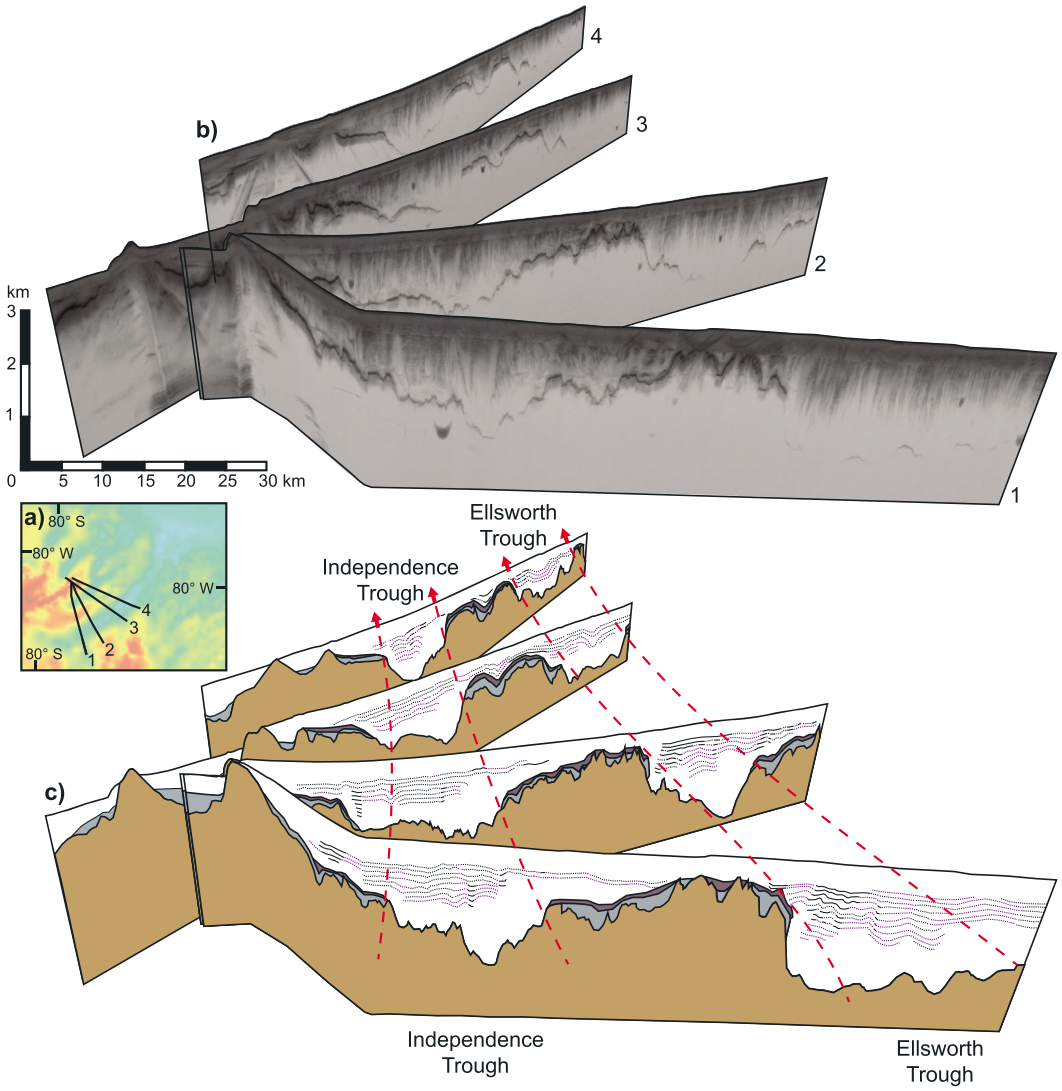

Figure 6. (a) Location of lines 1–4 in relation to the bed topography, derived from Bedmap2 [*Fretwell et al.*, 2013]. (b) Three-dimensional schematic diagram placing RES lines into approximate geographic/spatial context to highlight the morphology of Independence and Ellsworth Troughs, as well as the development of internal stratigraphy down flow. (c) Interpreted gross-scale structure of the two troughs, approximately marked by red dashed lines and flow direction arrows. Conformable layering is present above the highland plateaus which bound the troughs. The gradual inclination in bed elevation from Independence Trough to Independence Hills, coupled with the presence of basal ice zones and a thin ice column, suggests that there has been no recent transfer of ice from Independence Trough into Horseshoe Valley Trough.

often be subdivided into two distinct subunits, where the boundary between them is marked by an upper reflective interval. Although their formation requires further investigation, *Bingham et al*. [2015] suggest that their form could be attributable to changes in ice fabric, or contrasting physical, dielectric properties associated with a glacial/interglacial paleoclimatic switch.

4.2.1. Horseshoe Valley Trough

Basal ice units, up to 450 m thick, sit above the subglacial mountain ranges that delimit Horseshoe Valley Trough (Figure 3). These zones can be traced down flow on the southwestern side of the trough for at least 110 km, where they are clearly visible at a maximum depth of 500 m below sea level, but they cannot be found any more centrally or deeper within the trough itself. Discontinuous ice layers dominate the middle to lower ice column within Horseshoe Valley Trough, where the most disturbed and buckled englacial layers, with an ILCI value of 0–0.06, are found down the northeast flank of the trough (Figures 3 and 8). As discussed

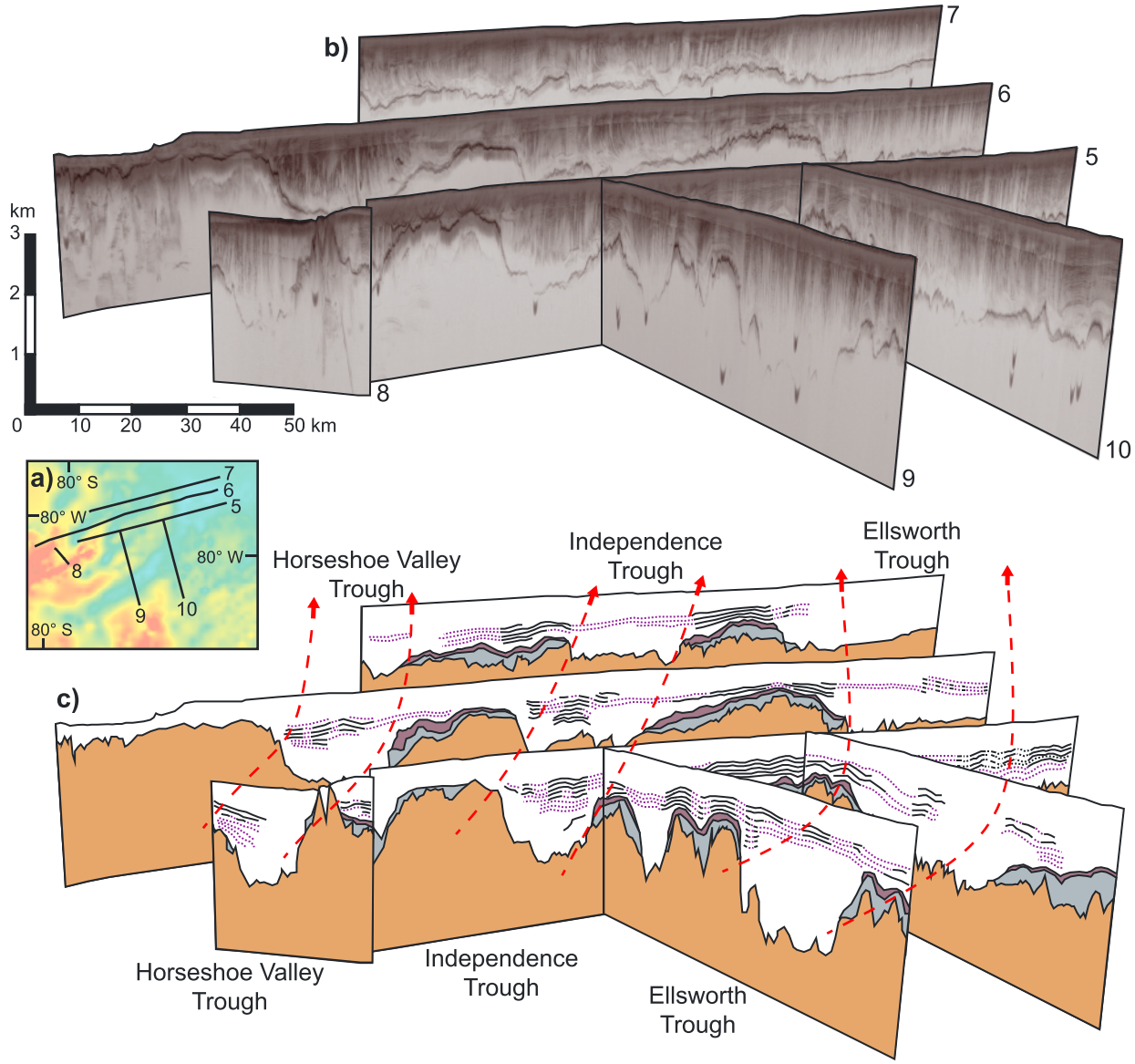

Figure 7. (a) Location of lines 5–10 in relation to the bed topography, derived from Bedmap2 [*Fretwell et al*., 2013]. (b) Three-dimensional schematic diagram to highlight the morphology of Horseshoe Valley, Independence and Ellsworth Troughs in the upper Institute Ice Stream catchment, as well as the development of internal stratigraphy down flow. (c) Interpreted gross-scale structure of the three troughs, approximately marked by the red dashed lines and flow direction arrows. Conformable layering is present above the highland plateaus which bound the troughs and in the upper 500 m of ice within Horseshoe Valley Trough. Disrupted isochrones are restricted to the deeper ice of Horseshoe Valley Trough and within Independence and Ellsworth Troughs.

in section 3.1 internal layers cannot be resolved within the southwestern side of the trough, as the aircraft took off and/or landed at this locality.

Continuous and parallel isochrones sit conformably above the deeper, more disrupted, and buckled ice layers within Horseshoe Valley Trough (Figure 3). These 20 km wide surface-conformable isochrones are observed in the upper 20% of the ice sheet column where they form an ~500 m thick sequential ice package. These continuous layers can be traced down flow in numerous radargrams, and through ILCI analysis, for at least 90 km, where the layers become increasingly apparent and abundant as the basal topography becomes elevated and the trough margins widen. As the internal stratigraphy of the entire ice column is averaged during ILCI analysis the thick package of disrupted and discontinuous englacial layering dominates the return of ILCI values along Horseshoe Valley Trough (Figure 8). ILCI values of 0 and 0.1 along the southwestern side

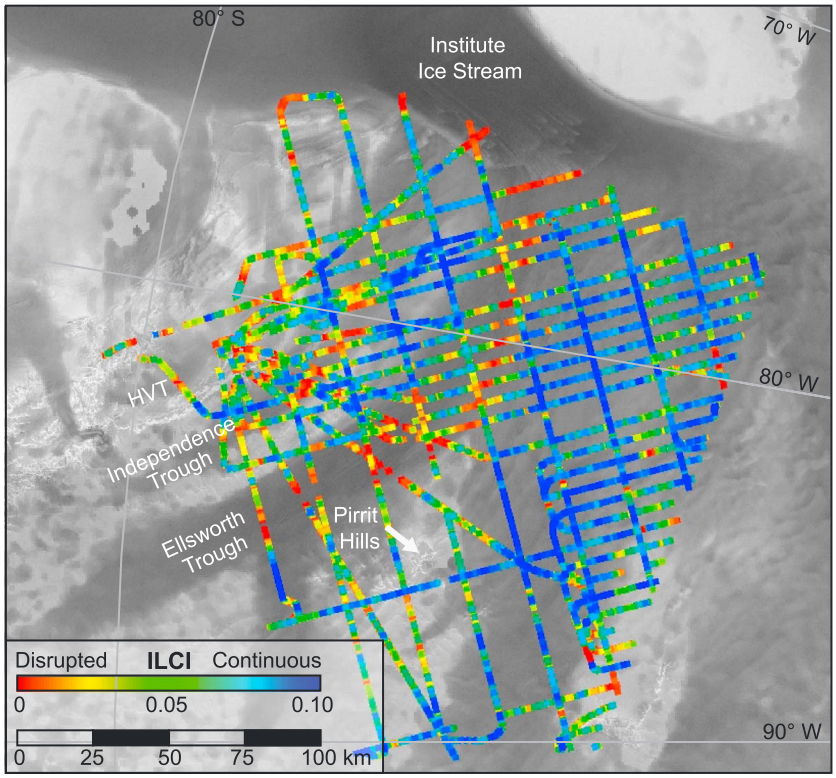

Figure 8. Results of the Internal Layer Continuity Index (ILCI) from several flight lines over the Institute Ice Stream upper catchment near the Ellsworth Mountains. Background shows surface ice-flow velocity from MEaSUREs [*Rignot et al.*, 2011a] in grey scale, superimposed onto RADARSAT mosaic [*Haran et al.*, 2006]. Low ILCI values (<0.06), representing disrupted englacial layering, dominate ice flows within Horseshoe Valley Trough (HVT), Independence Trough, and Ellsworth Trough as well as Institute Ice Stream. High ILCI values (>0.06), representing continuous layering, are located above the subglacial highlands which delimit the three troughs.

of Horseshoe Valley reflect an absence of apparent internal layering, which in this case is simply a function of data acquisition constraints (i.e., acquisition during aircraft takeoff and landing).

Although hard to distinguish precisely in all RES transects due to the scale at which they are presented in Figures 3, 4, 6, and 7, largely vertical whirlwind features are also visible within the ice of Horseshoe Valley Trough. Within the better resolved northern side of the ice flow, the whirlwinds appear to span the entire height of the ice sheet column (although processing steps largely prevent the upper 200 samples from being imaged), where they cut through both continuous and discontinuous internal layering. The whirlwinds, which generally tend to extend vertically downward from the surface or near surface, are sometimes curved or subvertical (see Figure 5 for a detailed example). This often occurs on a smaller scale, where the whirlwinds interface with the upper boundary of the basal ice units [*Ross and Siegert*, 2014].

4.2.2. Independence Trough

RES of Independence Trough reveals strong radar returns within the top 50% (800 m) of the ice column, where ice within the trough is dominated by disrupted englacial stratigraphy (Figure 4) which repeatedly exhibits an ILCI index <0.06. Figures 6–8 demonstrate the abundance of this stratified englacial layer buckling across flight lines of all orientations. They also show that the buckled ice layers become progressively less discernible down valley, likely as a function of enhanced ice flow and intense disruption of englacial stratigraphy on approach to the fast-flowing IIS trunk. Although low ILCI values dominate the majority of the ice flow within Independence Trough, ILCI values in excess of 0.06 (reflecting continuous layering) are recorded within the upper reaches of the trough, where they are often coincident with subglacial plateaus which have a relatively smooth basal topography (Figures 6–8).

Basal ice units are not found centrally within Independence Trough, but they can be seen at the trough margins, where the ~100 m thick packages drape over the subglacial highlands, spanning an elevation range

of 1250 m. Like in Horseshoe Valley Trough, a dense network of whirlwinds is also observed within the ice flow of Independence Trough. These whirlwinds are found above the higher-elevation subglacial mountain ranges and associated basal ice units (e.g., Figure 5), where they have been located in ice as thin as 600 m and in ice as thick as 1500 m, within Independence Trough.

4.2.3. Ellsworth Trough

The entire length of Ellsworth Trough is dominated by subparallel, buckled isochrones which are visible within the uppermost 1000 m of the ice column, to a maximum depth of 250 m below current sea level, beneath which the radar did not resolve internal layering due to signal attenuation (a function of the 2600 m+ ice thickness and the existence of warm ice within the lower ice column). ILCI results reveal the greatest percentage of low to intermediate ILCI values (0–0.6) within Ellsworth Trough (Figure 8), quantitatively confirming that this trough contains the most abundant unresolved and disrupted internal stratigraphy of all the southwestern IIS tributaries. Although continuous layering is clearly distinguishable above the highland plateau of the Pirrit Highlands, which delimit the southwestern extent of the trough (Figure 8), very few continuous layers are found within Ellsworth Trough itself. This is particularly evident from the ILCI results (Figure 8), where values $<$0.6 representing disrupted englacial layering are found down the center of the trough, while intermediate to high ILCI values (0.6–0.10) are located near the trough margins.

Beneath the surface-conformable layers of the Pirrit Subglacial Highlands basal ice units are clearly visible down the length of the mountainous ridge (Figure 7), where they typically reach thicknesses in excess of 200 m, with a maximum thickness of 850 m (recorded in a small trough within the upper reaches of the highland area). The most frequent and elongate whirlwinds of our entire study region are also found in Ellsworth Trough, where the nearly vertical whirlwind features display longitudinal continuity down flow. Although smaller, more infrequent, and less distinctive, whirlwinds are also resolved over some areas of the Pirrit Highlands.

4.3. Surface Velocity and Surface Features

Satellite remotely sensed ice velocity data [*Rignot et al*., 2011a] reveal spatially variable ice-flow speeds within the upper catchment area of IIS tributaries, in and around the Ellsworth Mountains. The slowest ice-flow speeds of $<9\ \mathrm{m\,a^{-1}}$ are recorded above high-elevation subglacial plateaus and mountain ranges, while faster ice flow is recorded within the deep subglacial troughs which feed the IIS trunk, where current flow speeds reach $415\ \mathrm{m\,a^{-1}}$. Ice within Horseshoe Valley Trough maintains the slowest average flow speeds of $12\ \mathrm{m\,a^{-1}}$ (Figure 3), permitting the preservation of early-mid-Holocene ice. Ages quoted here and henceforth are approximate and estimated using age-depth modeling calculations at Bungenstock Ice Rise, which suggest that ice at 40% ice thickness is ~4000 years old [*Siegert et al*., 2013], as there is currently no dating control across the upper IIS catchment. Ice in Independence Trough currently reaches flow speeds up to $35\ \mathrm{m\,a^{-1}}$ (Figure 4). Assuming average flow speeds $\geq 35\ \mathrm{m\,a^{-1}}$ it can be deduced that ice in Independence Trough is unlikely to contain ice deposited earlier than the mid-Holocene. Even greater advection of early to mid-Holocene ice is expected within Ellsworth Trough, where tributary flow speeds of ~70–130 $\mathrm{m\,a^{-1}}$ are currently recorded. Here distinctive surface flow stripes, orientated parallel to ice flow, are clearly identified on satellite imagery and ice velocity maps (Figures 4c and 4d). Recent investigations by *Glasser and Gudmundsson* [2012] and *Glasser et al*. [2015] suggest that these longitudinal features are likely to be the surface expression of simple shear and lateral compression, in this case originating from the confluence point of tributary flows entering Ellsworth Trough.

5. Discussion

5.1. Current Configuration of Institute Ice Stream and Its Tributaries

In its present configuration, two main tributaries feed the southwestern catchment of IIS; these tributaries carry ice along Independence and Ellsworth Troughs to the main trunk of IIS and ultimately the FRIS, entraining the flow of smaller tributaries, including ice that has originated from Horseshoe Valley.

Horseshoe Valley Trough is characterized at its upper end by the Horseshoe Valley overdeepened basin, where maximum measured ice thickness is in excess of 2000 m. This ice thickness is not maintained down valley, reducing to ~1400 m, and later ~750 m, when the ice is driven up topographic steps in the bed near the valley mouth (Figure 7). Surface-conformable ice layers dominate the upper 20% of the ice column in

all transects; this continuity reflects the current slow flow speeds within Horseshoe Valley Trough which amount to ~12 m a^{-1}. However, disrupted internal layers, visible within the RES transects (Figures 3 and 7) and ILCI plot (Figure 8), imply former enhanced ice flow within the trough. As surface-conformable stratigraphy blankets the buckled ice layers it can be deduced that at some time the faster-than-present ice flow experienced a switch-off, fossilizing the enhanced flow features (buckled layers). The continuous isochrones beneath the surface of Horseshoe Valley Trough, combined with the preservation of conformable stratigraphy and basal ice zones above the subglacial mountains that delimit Horseshoe Valley Trough, provide evidence for topographically confined and relatively stagnant isolated ice flow throughout the Holocene. The Horseshoe Valley Trough evidence suggests that the switch from enhanced to stagnant flow occurred pre-Holocene, so enhanced ice flow in this system is likely to predate the major changes in regional ice flow associated with the shutdown of ice streaming across Bungenstock Ice Rise [*Siegert et al*., 2013].

Confined by steep mountain ranges along its length, the ~2200 m thick ice flow within Independence Trough is dominated by buckled ice layers which are visible in the top 50% of the ice column, within flight lines of all orientations (Figures 6–8). These buckled layers become less discernible on approach to the main IIS trunk (Figures 6 and 7), as a function of enhanced ice-flow speeds and increased strain rates. Unlike the ice within Horseshoe Valley Trough, there is no evidence for recent continuous englacial layering within Independence Trough, even though similar flow speeds of 15 m a^{-1} are recorded within the upper reaches of the trough. This suggests that the buckled ice layers within Independence Trough are younger than those in Horseshoe Valley Trough, implying a more recent slowdown of ice flow here.

Low ILCI values are recorded throughout the topographically constrained Ellsworth Trough, where discontinuous and buckled ice layers dominate the uppermost 1000 m of the ice column (note that detailed internal layering is poorly resolved at greater depths). These disrupted layers can be found in radargrams of all orientations (Figures 4, 6, 7, and 8). This extensive deformation is largely attributed to the relatively high ice surface flow speeds of 70–130 m a^{-1} (calculated from *Rignot et al*. [2011a]). Surface flow stripes correlate well to ILCI values, where the lowest ICLI values and surface flow stripes are recorded near the ice stream margin (Figures 4 and 8) where shear stress is high. A similar phenomenon is found in Whillans and the Carlson Inlet Ice Stream feature [*Raymond et al*., 2006; *King*, 2011], as well as IIS toward its upper confluence with MIS [*Bingham et al*., 2015] where the greatest disruption of internal layering is found along the lateral shear margins. These features define a constant direction of shear within the ice of Ellsworth Trough, which given the topography of the trough [*Ross et al*., 2014], is likely to have existed over significant intervals of geological time.

5.2. Evidence for Former Enhanced Ice Flow and Ice-Flow Reorganization

Intensely buckled and discontinuous ice layers and whirlwinds in Independence and Ellsworth Troughs provide evidence for former and present enhanced ice flows within these two main tributaries of IIS. However, continuous stratigraphy and the presence of basal ice zones above neighboring subglacial mountain ranges suggest that the ice flow has remained topographically constrained during periods of both slower and enhanced ice flows. This topographic confinement limits the potential for water piracy or ice-flow reorganization in the upper IIS catchment, as has been speculated in other ice streams, most notably for the currently stagnant Kamb Ice Stream [*Jacobel et al*., 1996; *Anandakrishnan and Alley*, 1997], although it does permit on-and-off streaming of tributary flow. Although disrupted isochrones are qualitatively and quantitatively recorded in Horseshoe Valley Trough the presence of 500 m of surface-conformable stratigraphy beneath the ice surface, coupled with present ice-flow speeds of 7 m a^{-1}–16 m a^{-1}, implies that the ice within Horseshoe Valley Trough has not experienced enhanced ice flow for some time, probably since at least the mid-Holocene.

5.3. Former Ice Sheet Configuration, With Respect to Bungenstock Ice Rise

Tectonically controlled bedrock folds beneath IIS catchment [*Jordan et al*., 2013] govern the location of deep trough systems and high mountain ranges in and around the Ellsworth Mountains, which facilitate channelized ice flow from the WAIS interior to the FRIS in the Weddell Sea. *Bingham et al*. [2015] suggested that the current configuration of topographically confined IIS tributary flows also reflects the spatial configuration of ice flow throughout the Holocene (and possibly earlier). Although the topographic constraints of the IIS tributaries mean that they are unable to migrate, buckled isochrones and whirlwind features within ice flows

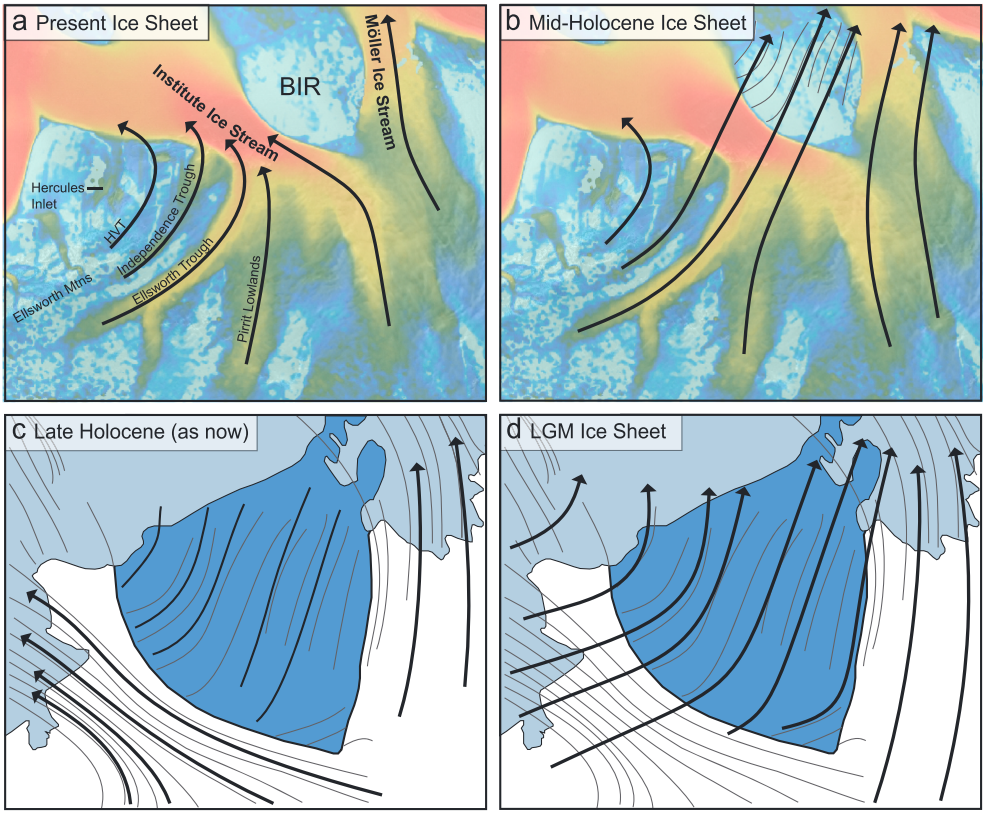

Figure 9. Schematic model of ice sheet change with respect to Bungenstock Ice Rise. (a) The current glaciological situation with ice flow indicated by arrows. (b) Mid-Holocene ice sheet, where northeastward ice flow dominates the region, crosscutting the present-day trunk of the Institute Ice Stream. (c) Late Holocene (as now) ice sheet flow described by *Siegert et al*. [2013] in which ice flow over Bungenstock Ice Rise becomes stagnant, thus leading to the present-day ice sheet configuration. (d) Last Glacial Maximum ice sheet hypothesized by *Siegert et al*. [2013]. Our interpretation in Figure 9b refines flow paths and their relative ages (mid-Holocene instead of LGM), as well as indicating minimal flow from Horseshoe Valley Trough toward Bungenstock Ice Rise.

of the Horseshoe Valley and Independence Troughs evidence former enhanced ice flow in presently slow-flowing tributaries, indicating a switch-off of past enhanced ice flow. Enhanced ice flow through Independence and Ellsworth Troughs during the mid-Holocene to late Holocene would have been conducive to driving ice flow across the IIS and the region now covered by Bungenstock Ice Rise (Figure 9), making these troughs strong candidates for contributing the ice flux necessary to facilitate paleo-ice streaming across what is currently a slow-flowing ice rise [*Siegert et al*., 2013]. The occurrence of buckled and disrupted layering at depth in Independence Trough supports this suggestion by providing evidence for former enhanced flow in a trough that is currently flowing slowly.

As surface-conformable stratigraphy dominates the upper ice column within Horseshoe Valley it is unlikely that flow from Horseshoe Valley Trough contributed significantly to the streaming flow over Bungenstock Ice Rise. This is likely to be a function of the topographically constrained nature of Horseshoe Valley Trough, as the high Ellsworth Mountains to the southeast largely block the ingress of the WAIS in this area, and subglacial topography at the trough mouth encourages the diversion of flow into Hercules Inlet (Figure 9b). However, as buckled ice layers have been preserved in the middle to lower half of the ice column in Horseshoe Valley Trough, it is proposed that changes within the flow of this tributary may have occurred earlier than the mid-Holocene. Assuming advection of the buckled englacial layers at a current average velocity of 12 m a^{-1}, early Holocene buckles would still be present in Horseshoe Valley Trough. The late Holocene deceleration of flow across Bungenstock Ice Rise previously inferred by *Siegert et al*. [2013] may therefore represent just one relatively local component of wider regional changes to ice flow that have occurred across IIS and MIS catchments as the WAIS has thinned since the LGM.

Stagnation of Bungenstock Ice Rise is the main hypothesis for the present-day configuration of IIS [*Bingham et al*., 2015]. The resultant reorganization of flow and switch-on of the main IIS trunk would have rerouted and/or switched off ice flow exiting the deep trough systems of the IIS upper catchment (e.g., Independence Trough), and led to grounding line migration and the diversion of flow across the FRIS, in an ice-flow configuration akin to that we see today (Figure 9).

6. Conclusion

Airborne radio echo sounding investigations of three Institute Ice Stream tributaries, sourced from and transecting the Ellsworth Subglacial Highlands, provide evidence for heterogeneous ice stream behavior and Holocene flow dynamics. It is likely that Independence and Ellsworth Troughs acted as source areas for the mid-Holocene to late-Holocene enhanced flow recorded in the Bungenstock Ice Rise [*Siegert et al*., 2013]. The internal stratigraphy of ice flowing along Independence and Ellsworth Troughs suggests that they may have acted independently of one another, undergoing asynchronous enhanced ice flow or a slowdown in ice streaming. The earliest evidence for enhanced ice flow, believed to have occurred ~4000 years ago [*Siegert et al*., 2013], is found in Horseshoe Valley Trough, where buckled and discontinuous isochrones are surveyed beneath a 500 m thick sequence of parallel, surface-conformable isochrones. Evidence for changing ice-flow velocities, possibly occurring more than ~400 years before present [*Siegert et al*., 2013], can be found within the topographically confined Independence and Ellsworth Troughs where strongly deformed isochrones represent former enhanced ice flow through each trough, which would have allowed ice to traverse the main trunk of the IIS and flow over the region now covered by Bungenstock Ice Rise.

These findings indicate dynamic changes in ice-flow velocity, which affected the interior parts of the Weddell Sea Sector. Our observations are consistent with the hypothesis that the Last Glacial Maximum and Holocene drainage pathways within the Weddell Sea sector of the West Antarctic Ice Sheet were different from those of the present day [*Larter et al*., 2012; *Siegert et al*., 2013].

Acknowledgments
Radar data used for this article are available at the NERC Airborne Geophysics Data Portal: https://secure.antarctica.ac.uk/data/aerogeo/access/imafi/. Note that original line numbers are required to access the specific data used in this paper; this information is available in Figure S1 in the supporting information. Data related to surface ice velocity from MEaSUREs [*Rignot et al*., 2011a], bed elevation, derived from Bedmap2 [*Fretwell et al*., 2013], and mosaic imagery (LIMA, MODIS, and RADARSAT) can be downloaded from the Quantarctica data set: http://www.quantarctica.org/downloads/. Financial support for the Institute and Möller Ice Stream Project was provided by the UK Natural Environment Research Council (NERC) Antarctic Funding Initiative grant NE/G013071/1. Project work was funded by NERC standard grants NE/I027576/1, NE/I025840/1, NE/I024194/1, and NE/I025263/1. We thank the British Antarctic Survey for the field logistics support.

References

Anandakrishnan, S., and R. B. Alley (1997), Stagnation of ice stream C, West Antarctica by water piracy, *Geophys. Res. Lett.*, *24*, 265–268, doi:10.1029/96GL04016.

Bentley, M. J., C. J. Fogwill, A. M. Le Brocq, A. L. Hubbard, D. E. Sugden, T. J. Dunai, and S. P. H. T. Freeman (2010), Deglacial history of the West Antarctic Ice Sheet in the Weddell Sea embayment: Constraints on past ice volume change, *Geology*, *38*, 411–414, doi:10.1130/G30754.1.

Bindschadler, R. A., D. G. Vaughan, and P. Vornberger (2011), Variability of basal melt beneath the Pine Island Glacier ice shelf, West Antarctica, *J. Glaciol.*, *57*, 581–595, doi:10.3189/002214311797409802.

Bingham, R. G., M. J. Siegert, D. A. Young, and D. D. Blankenship (2007), Organized flow from the South Pole to the Filchner-Ronne ice shelf: An assessment of balance velocities in interior East Antarctica using radio echo sounding data, *J. Geophys. Res.*, *112*, F03S26, doi:10.1029/2006JF000556.

Bingham, R. G., D. M. Rippin, N. B. Karlsson, H. F. J. Corr, F. Ferraccioli, T. A. Jordan, A. M. Le Brocq, K. C. Rose, N. Ross, and M. J. Siegert (2015), Ice-flow structure and ice-dynamic changes in the Weddell Sea sector of West Antarctica from radar images internal layering, *J. Geophys. Res. Earth Surface*, *120*, 655–670, doi:10.1002/204JF003291.

Bradley, S. L., R. C. A. Hindmarsh, P. L. Whitehouse, M. J. Bentley, and M. A. King (2015), Low post-glacial rebound rates in the Weddell Sea due to late Holocene ice-sheet readvance, *Earth Planet. Sci. Lett.*, *413*, 79–89, doi:10.1016/j.epsl.2014.12.039.

Catania, G. A., T. A. Scambos, H. Conway, and C. F. Raymond (2006), Sequential stagnation of Kamb Ice Stream, West Antarctica, *Geophys. Res. Lett.*, *33*, L14502, doi:10.1029/2006GL026430.

Clark, P. U., A. S. Dyke, J. D. Shakun, A. E. Carlson, J. Clark, B. Wohlfarth, J. X. Mitrovica, S. W. Hostetler, and A. Marshall McCabe (2009), The last glacial maximum, *Science*, *325*, 710–714, doi:10.1126/science.1172973.

Conway, H., G. Catania, C. F. Raymond, A. M. Gades, T. A. Scambos, and H. Engelhardt (2002), Switch of flow direction in an Antarctic Ice Stream, *Nature*, *419*, 465–467, doi:10.1038/nature01081.

Corr, H., F. Ferraccioli, N. Frearson, T. A. Jordan, C. Robinson, A. Armadillo, G. Caneva, E. Bozzo, and I. E. Tabacco (2007), Airborne radio-echo sounding of the Wilkes Subglacial Basin, the Transantarctic Mountains, and the Dome C Region, *Terra Antart. Rep.*, *13*, 55–63.

Drews, R., M. D. Steinhage, and O. Eisen (2013), Characterizing the glaciological conditions at Halvfarryggen ice dome, Dronning Maud Land, Antarctica, *J. Glaciol.*, *59*, 9–20, doi:10.3189/2013JoG12J134.

Fogwill, C. J., C. S. M. Turney, N. R. Golledge, D. H. Rood, K. Hippe, L. Wacker, R. Wieler, E. B. Rainsley, and R. S. Jones (2014), Drivers of abrupt Holocene shifts in West Antarctic ice stream direction determined from combined ice sheet modelling and geologic signatures, *Antarct. Sci.*, *26*, 674–686, doi:10.1017/S0954102014000613.

Fretwell, P., et al. (2013), Bedmap2: Improved ice bed, surface and thickness datasets for Antarctica, *Cryosphere*, *7*, 375–393, doi:10.5194/tc-7-375-2013.

Glasser, N. F., and G. H. Gudmundsson (2012), Longitudinal surface structures (flowstripes) on Antarctic glaciers, *Cryosphere*, *6*, 383–391, doi:10.5194/tc-6-383-2012.

Glasser, N. F., S. J. A. Jennings, M. J. Hambrey, and B. Hubbard (2015), Origin and dynamic significance of longitudinal structures ("flow stripes") in the Antarctic Ice Sheet, *Earth Surf. Dyn.*, *3*, 239–249, doi:10.5194/esurf-3-239-2015.

Haran, T., J. Bohlander, T. Scambos, T. Painter, and M. Fahnestock (2006), *MODIS Mosaic Image of Antarctica*, Natl. Snow and Ice Data Cent., Digital media, Boulder, Colo.

Holschuh, N., K. Christianson, and S. Anandakrishnan (2014), Power loss in dipping internal reflectors, imaged using ice-penetrating radar, *Ann. Glaciol.*, *55*, 49–56, doi:10.3189/2014AoG67A005.

Hulbe, C. L., and M. A. Fahnestock (2007), Century-scale discharge stagnation and reactivation of the Ross Ice Streams, West Antarctica, *J. Geophys. Res.*, *112*, F03S27, doi:10.1029/2006JF000603.

Jacobel, R. W., T. A. Scambos, C. F. Raymond, and A. M. Gades (1996), Changes in the configuration of ice stream flow from the West Antarctic Ice Sheet, *J. Geophys. Res.*, *101*, 5499–5504, doi:10.1029/95JB03735.

Jordan, T. A., F. Ferraccioli, N. Ross, H. F. J. Corr, P. T. Leat, R. G. Bingham, D. M. Rippin, A. M. Le Brocq, and M. J. Siegert (2013), Inland extent of the Weddell Sea Rift imaged by new aerogeophysical data, *Tectonophysics*, *585*, 137–160, doi:10.1016/j.tecto.2012.09.010.

Joughin, I., and J. L. Bamber (2005), Thickening of the ice stream catchments feeding the Filchner-Ronne Ice Shelf, Antarctica, *Geophys. Res. Lett.*, *32*, L17503, doi:10.1029/2005GL023844.

Karlsson, N. B., D. M. Rippin, D. G. Vaughan, and H. F. J. Corr (2009), The internal layering of Pine Island Glacier, West Antarctica, from airborne radar-sounding data, *Ann. Glaciol.*, *50*, 141–146.

Karlsson, N. B., D. M. Rippin, R. G. Bingham, and D. G. Vaughan (2012), A "continuity index" for assessing ice-sheet dynamics from radar-sounded internal layers, *Earth Planet. Sci. Lett.*, *335–336*, 88–94, doi:10.1016/j.epsl.2012.04.034.

King, E. C. (2011), Ice stream or not? Radio-echo sounding of the Carlson Inlet, West Antarctica, *Cryosphere*, *5*, 907–916, doi:10.5194/tc-5-907-2011.

Larter, R. D., A. G. C. Graham, C.-D. Hillenbrand, J. A. Smith, and J. A. Gales (2012), Late Quaternary grounded ice extent in the Filchner Trough, Weddell Sea, Antarctica: New marine geophysical evidence, *Quat. Sci. Rev.*, *53*, 111–122, doi:10.1016/j.quascirev.2012.08.006.

Raymond, C. F., G. A. Catania, N. Nereson, and C. J. van der Veen (2006), Bed radar reflectivity across the north margin of the Whillans Ice Stream, West Antarctica, and implications for margin processes, *J. Glaciol.*, *52*, 3–10, doi:10.3189/172756506781828890.

Rignot, E., J. Mouginot, and B. Scheuchl (2011a), *MEaSUREs InSAR-Based Antarctica Ice Velocity Map*, NASA DAAC at the Natl. Snow and Ice Data Cent., Boulder, Colo., doi:10.5067/MEASURES/CRYOSPHERE/nsidc-0484.001.

Rignot, E., J. Mouginot, and B. Scheuchl (2011b), Ice flow of the Antarctic Ice Sheet, *Science*, *333*, 1427–1430, doi:10.1126/science.1208336.

Rippin, D. M., M. J. Siegert, and J. L. Bamber (2003), The englacial stratigraphy of Wilkes Land, East Antarctica, as revealed by internal radio-echo sounding layering, and its relationship with balance velocities, *Ann. Glaciol.*, *36*, 189–196, doi:10.3189/172756403781816356.

Ross, N., and M. Siegert (2014), Concentrated englacial shear over rigid basal ice, West Antarctica: Implications for modelling and ice sheet flow, *Geophys. Res. Abstr.*, *16*, EGU2014-5568.

Ross, N., R. G. Bingham, H. F. J. Corr, F. Ferraccioli, T. A. Jordan, A. Le Brocq, D. M. Rippin, D. Young, D. D. Blankenship, and M. J. Siegert (2012), Steep reverse bed slope at the grounding line of the Weddell Sea sector in West Antarctica, *Nat. Geosci.*, *5*, 393–396, doi:10.1038/NGEO1468.

Ross, N., T. A. Jordan, R. G. Bingham, H. F. J. Corr, F. Ferraccioli, A. Le Brocq, D. M. Rippin, A. P. Wright, and M. J. Siegert (2014), The Ellsworth Subglacial Highlands: Inception and retreat of the West Antarctic Ice Sheet, *Geol. Soc. Am. Bull.*, *126*, 3–15, doi:10.1130/B30794.1.

Sandmeier Scientific Software (2012), ReflexW, version 6.1.1. [Available to download from http://www.sandmeier-geo.de/download.html.]

Siegert, M. J., A. J. Payne, and I. Joughin (2003), Spatial stability of Ice Stream D and its tributaries, West Antarctica, revealed by radio-echo sounding and interferometry, *Ann. Glaciol.*, *37*, 377–382, doi:10.3189/172756403781816022.

Siegert, M., N. Ross, H. Corr, J. Kingslake, and R. Hindmarsh (2013), Late Holocene ice flow reconfiguration in the Weddell Sea sector of West Antarctica, *Quat. Sci. Rev.*, *78*, 98–107, doi:10.1016/j.quascirev.2013.08.003.

Vaughan, D. G., et al. (2013), Observations: Cryosphere, in *Climate Change 2013: The Physical Science Basis*, Cambridge Univ. Press, Cambridge, U. K., and New York.

Wright, A. P., et al. (2014), Sensitivity of the Weddell Sea sector ice streams to sub shelf melting and surface accumulation, *Cryosphere*, *8*, 2119–2134, doi:10.5194/tc-8-2119-2014.